Status and plans of the ITER Pulse Design Simulator

M. Schneider[1], J.F. Artaud[2], M. Bellouard[1,3], S. Blokhuizen[4], J. Citrin[5], M. Dubrov[1], B. Faugeras[6], A. Fernando[5], G. Gros[2,6], R. Nouailletas[2], O. Hoenen[1], R.A. Pitts[1], T. Ravensbergen[1], M. Sanders[4], M. Sebregts[4], D. van Vugt[4], A. Vu[1]

[1] ITER Organization, Route de Vinon-sur-Verdon, CS 90 046, 13067 St. Paul-lez-Durance, France - [2] CEA, IRFM, F-13108 Saint Paul-lez-Durance, France - [3] Aix-Marseille Université, CNRS, Centrale Marseille, M2P2 UMR 7340, Marseille, France - [4] Ignition Computing B.V. Torenallee 30-12, 5617BD Eindhoven, The Netherlands - [5] Google DeepMind London, UK - [6] Université Côte d'Azur, CNRS, INRIA Castor, LJAD, F-06108 Nice, France

1. Introduction

The ITER Pulse Design simulator (PDS) is an open-source tool being developed by ITER Organization to design, optimize and validate pulses before operating them on the machine. The development of such a tool is essential for preparing ITER operation, including the training of future session leaders. The initial version of the PDS includes the NICE Free-Boundary Equilibrium (FBE) code [1] coupled with the METIS [2] and TORAX [3] transport solvers. The technical choices and approach adopted for the development of the ITER PDS follows the same development path as the WEST flight simulator [4], and the JT-60SA pulse design simulator [5]. This paper presents the status of the ITER PDS and the foreseen next steps for its development. Some initial results of self-consistent simulations between transport and Electron Cyclotron Heating (ECH) are also presented for a 15 MA / 5.3T scenario of the ITER Start of Research Operation (SRO) phase.

2. Main components of the ITER PDS

The ITER PDS is developed as two different components:

1) A pulse editor (or pulse planner), to configure the desired pulse based on waveform and plasma shape editors to deliver an initial set of waveforms, relying on a static inverse mode calculation of the FBE code, to deduce coil currents based on the desired plasma shape, as shown in Fig. 1.

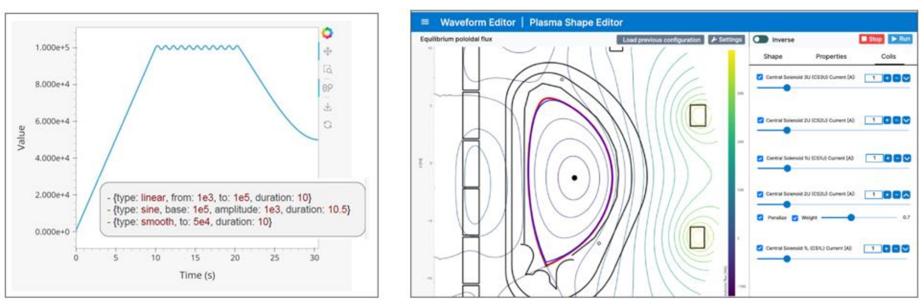

Fig. 1 –Waveform and plasma shape editor developed for the ITER PDS.

2) A pulse simulator relying on a direct mode calculation of the FBE code, calculating the flux map and consumption based on a set of coil currents, combined with magnetic controllers to check the viability of a pulse and estimate the magnetic flux consumption, essential to evaluate long pulse operation capabilities. Magnetic controllers are provided by the Plasma Control System Simulation Platform PCSSP [6], to control the plasma shape, current and vertical stability.

Several other models and workflows are being integrated within the PDS, e.g. for Heating and Current Drive (H&CD) sources [7,8], or to describe the boundary plasma, allowing estimates of the peak divertor target heat flux in response to fuel injection, impurity seeding and upstream separatrix scrape-off layer parameters for core-boundary integration [9].

3. Coupling strategy and technical implementation

To offer the best flexibility and modularity of the coupled models, the ITER PDS uses the IMAS standard [10] associated with the Muscle3 (M3) Persistent Actor Framework (PAF) [11] to enable easy communication between models implemented in different programming languages (C++, Fortran, Python and Matlab-Simulink). The M3 PAF allows flexibility in terms of coupling patterns between models, from a simple chain (dispatch), a typical micro-macro coupling (call and release) or a tight coupling between overlapping models (interaction). It allows the use of checkpoints to restart a simulation from a given state in case of failure (either from a wrong waveform evolution or from a crash of the computer) as well as timescale bridges to couple models describing physics on different time and space scales. Such concepts are illustrated e.g. in Fig. 2 in the context of the workflow being developed for Neoclassical Tearing Mode (NTM) control studies in the ITER PDS [12]. Some results of NTM control studies are displayed in Fig. 3 where the capability to stabilize a q=2 magnetic islands has been assessed for various initial steering angles of EC mirrors in an SRO L-mode 15 MA / 5.3T hydrogen scenario.

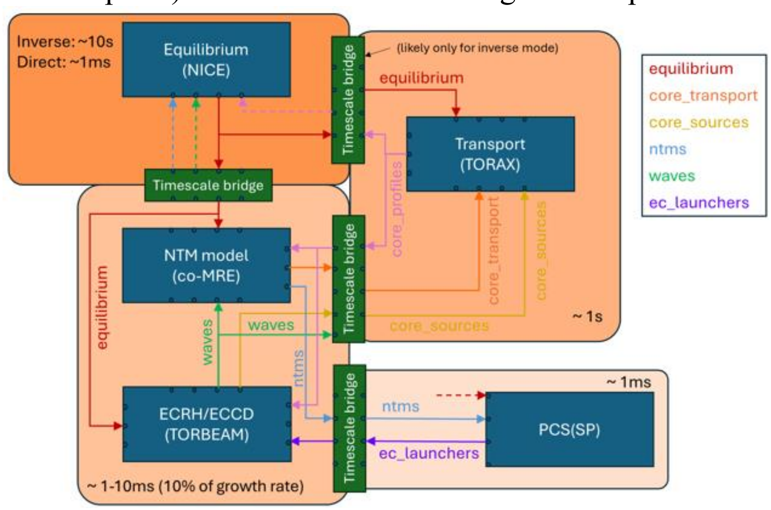

Fig. 2 – Coupling scheme in the workflow for NTM control with the various involved timescales

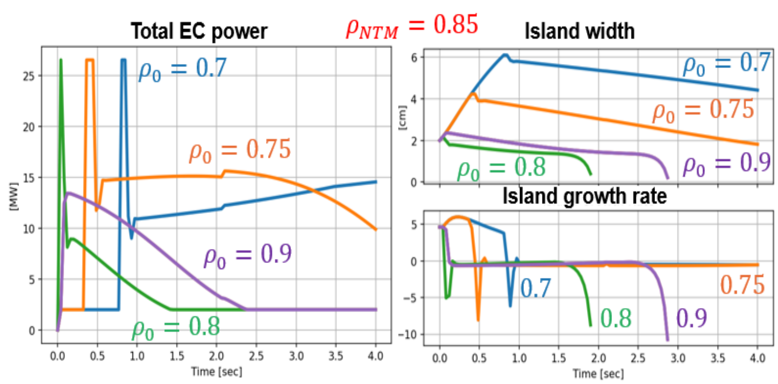

Fig. 3 – Dynamics of EC stabilization power and q=2 island width and growth rate for various initial location of EC mirrors on an ITER SRO 15 MA / 5.3 T scenario.

4. Initial results for scenarios of ITER Start of Research Operation (SRO) phase

As a first demonstration of PDS modelling capabilities, a comparison of the ECH absorption efficiency between O1 and X1 polarization in an ITER SRO 15 MA / 5.3T scenario has been performed. The goal is to find the optimal polarization during the early ramp-up and late ramp-down: X1 can indeed absorb at low density due to that its cut-off layer is close to the resonance layer (cf. fig. 4), while O1 absorption is known to be less efficient than X1 at low density and temperature [13]. The modelling has been carried out with the NICE inverse mode coupled to the TORAX transport solver using the Qualikiz Neural Network model QLKNN_7_11 [14]. In this simulation, heat and particle transport are activated together with current diffusion calculated by TORAX. The radiation level is estimated with Mavrin polynomial fits from ADAS, the neoclassical bootstrap current is evaluated using the Sauter model, and the ECH efficiency is simulated by TORBEAM [15]. The pulse is based on an existing DINA scenario [16] from which impurity fraction, initial profiles and edge boundary conditions are still prescribed.

The results indicate 100% ECH X1 absorption until ~25s in the early ramp-up, i.e. until the cut-off layer moves too far from the resonance for absorption to occur, while O1 absorption increases from 75% and 95% for the first 20s of the ramp-up. Given that non-absorbed EC power from O1 shine-through losses may be detrimental for the ITER first wall, especially for the SRO phase operating with a temporary inertially cooled first wall, using X1 polarisation for the early ramp-up and late ramp-down seems to be an optimal strategy. However, changing polarization for a given beam / gyrotron is expected to take 3 seconds, but since only a subset of gyrotrons is used for the reduced required EC power in the ramp-up and ramp-down phases, the gyrotrons which do not fire may be prepared in advance with the O1 polarization to take over after 25s of the ramp-up phase.

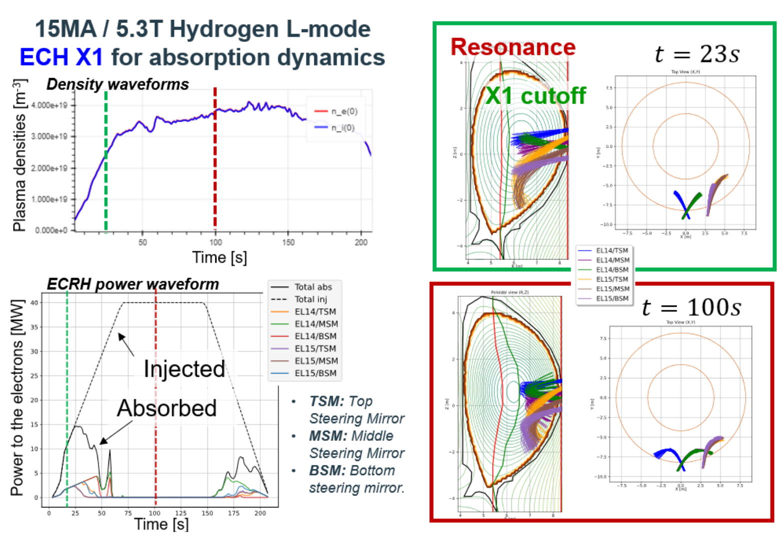

Fig. 4 – Dynamics of EC X1 absorption for an ITER SRO 15 MA / 5.3T scenario showing its possible use for early ramp-up and late ramp-down phases despite the X1 density cut-off layer.

5. Summary of the PDS status and next steps

The ITER PDS is still under development at the ITER Organization. Its static inverse mode is operational and reveals good agreement with the DINA transport suite for several ITER SRO scenarios. A first study of the dynamics of ECH absorption, based on self-consistent transport and H&CD modelling using the FBE static inverse mode, provides quantitative answers on the feasibility of X1 and O1 polarization of the EC wave during early ramp-up and late ramp-down of a 15 MA / 5.3 T scenario, essential to design optimal pulses for the ITER Research Plan. The PDS direct mode is still under development and is expected to deliver its first results in 2026-2027. The IMAS H&CD workflow is being integrated to provide the complete set of H&CD sources to the plasma. The SOLPS-NN surrogate model has also recently been integrated and is currently being tested [9]. The next development steps will be to implement segments in the PDS pulse editor and simulator to account for the transition between the various phases of the plasma, for a full end-to-end PDS simulation in direct evolutive mode with magnetic control. Fuelling associated with density control, together with tungsten transport modelling are the next natural steps for the PDS development. One short-term plan is to validate the PDS on the WEST tokamak, starting with its plasma shape editor, expected to be validated this year.

6. References

[1] B. Faugeras et al 2020, *An overview of the numerical methods for tokamak plasma equilibrium computation implemented in the NICE code.* Fus. Eng. Design 160 DOI/10.1016/j.fusengdes.2020.112020

[2] J.F. Artaud et al 2018 Nucl. Fusion 58 105001 DOI/10.1088/1741-4326/aad5b1

[3] J. Citrin et al 2024, *TORAX: A Fast and Differentiable Tokamak Transport Simulator in JAX* arXiv:2406.06718 DOI/10.48550/arXiv.2406.06718

[4] R. Nouailletas et al, SOFT, Dublin, *Development of a flight simulator for the WEST PCS* (2024)

[5] E. Joffrin et al, IAEA FEC 2025, PDS for JT-60SA DOI/10.2139/ssrn.6922039

[6] T. Ravensbergen et al 2023, Fus. Eng. Design 188 DOI/10.1016/j.fusengdes.2023.113440; T. Ravensbergen et al. / IFAC PapersOnLine 59-11 2025 192–197 DOI/10.1016/j.ifacol.2025.09.547

[7] M. Schneider et al 2021 Nucl. Fusion 61 126058, DOI/10.1088/1741-4326/ac34d8

[8] Z. Bian et al, SOFT conference, Aix-en-Provence, *Adaption of the ITER H&CD Workflow to MUSCLE3 for multi-scale integrated modelling* (2026)

[9] M. Karacsonyi, PSI conf, Regensburg, *Reduced boundary models for the ITER PDS* (2026), to be submitted to NME

[10] F. Imbeaux et al 2015 Nucl. Fusion 55 123006 DOI/10.1088/0029-5515/55/12/123006

[11] L.E. Veen and A. G. Hoekstra, *Easing Multiscale Model Design and Coupling with MUSCLE3*, ICCS 2020. ICCS 2020. DOI/10.1007/978-3-030-50433-5_33

[12] M. Schneider et al, EC-ECE workshop, *NTM control modelling with the ITER PDS* (2026)

[13] M. Bellouard et al, EC-ECE workshop, *Self-consistent modelling of transport and ECRH, applied to the ITER new baseline* (2026)

[14] https://github.com/google-deepmind/fusion_surrogates/

[15] E. Poli et al 2018, *TORBEAM 2.0, a paraxial beam tracing code for electron-cyclotron beams in fusion plasmas for extended physics applications* DOI/10.1016/j.cpc.2017.12.018

[16] R.R. Khayrutdinov, et al, JCoPh 109 193–201, *Studies of Plasma Equilibrium and Transport in a Tokamak Fusion Device with the Inverse-Variable Technique* (1993)